HYDRODYNAMICALLY SIMILAR ROLL STABILIZATION FINS FOR SHIP MODEL TESTS

DONALD R. MOYER
AND
ROBERT J. MICHAELS

HYDRODYNAMICALLY SIMILAR ROLL STABILIZATION FINS FOR SHIP MODEL TESTS

by

DONALD R. MOYER, LIEUTENANT, UNITED STATES NAVY

B.S., U. S. Naval Academy

(1951)

and

ROBERT J. MICHAELS, LIEUTENANT, UNITED STATES NAVY

B.S., U. S. Naval Academy

(1952)

SUBMITTED IN PARTIAL FULFILLMENT OF THE REQUIREMENTS

FOR THE DEGREE OF NAVAL ENGINEER

AND THE DEGREE OF

MASTER OF SCIENCE IN NAVAL ARCHITECTURE

AND MARINE ENGINEERING

at the

MASSACHUSETTS INSTITUTE OF TECHNOLOGY

May, 1958

HYDRODYNAMICALLY SIMILAR ROLL STABILIZATION FINS FOR SHIP MODEL TESTS

By Donald R. Moyer, Lt., U.S.N. and Robert J. Michaels, Lt., U.S.N.

Submitted to the Department of Naval Architecture and Marine Engineering on May 26, 1958 in partial fulfillment of the requirements for the degrees of Naval Engineer and Master of Science in Naval Architecture and Marine Engineering.

ABSTRACT

Model testing in general requires equivalency between model and ship Froude numbers. This results in Reynolds numbers appreciably lower for model than for ship, and leads to "scale effect" when dealing with fins or other lift producing devices. Basically, "scale effect" is the reduction of maximum obtainable lift coefficient and reduction of the angle of attack at which this maximum lift occurs for any given airfoil as Reynolds number is decreased.

This thesis investigates two approaches to the problem of obtaining equivalency of developed inclining moment and angle of breakdown between ship and model stabilization fins. The first approach consists of reducing the aspect ratio and increasing the area of the model fin. The second approach consists of using a geometrically similar fin constructed of perforated brass sheet and employing boundary layer control by suction. For the experimental work conducted in these investigations, the fins are installed on a model and the heel angle produced as a function of fin angle of attack is used as a measure of fin effectiveness.

The results of the experimental work indicate that both methods of approach offer feasible solutions to the problem. The authors recommend that a geometrically similar fin employing boundary layer control be used in preference to a low aspect ratio fin of increased area. This recommendation is based on the increased virtual mass effect of the low aspect ratio fin as compared with the geometrically similar fin.

Recommendations for refinement of experimental procedures and areas for further investigation are also made in the thesis.

Thesis Supervisor: Martin A. Abkowitz, Ph.D.
Title: Associate Professor of Naval Architecture

ACKNOWLEDGEMENTS

The authors are grateful to Professor Martin A. Abkowitz, Thesis Supervisor, for his many recommendations and invaluable assistance in the preparation of this thesis. His constant encouragement was a major factor in enabling the authors to carry their proposals to completion.

Special thanks must be given to Professor Joseph Bicknell, Thesis Advisor, whose assistance in the initial investigations bridged the gap between the Naval Architecture and Aeronautical Engineering aspects of this thesis. It was on his recommendation that the authors attempted the investigation of boundary layer control.

TABLE OF CONTENTS

TABLE OF CONTENTS (CONT.)

LIST OF FIGURES

LIST OF TABLES

NOMENCLATURE

Symbol	Meaning
AR	Aspect ratio
c_ℓ	Section lift coefficient
$c_\ell(max)$	Maximum section lift coefficient at angle of breakdown
C_L	Total lift coefficient
$C_L(max)$	Maximum total lift coefficient at angle of breakdown
C_q	Dimensionless pumping rate coefficient
d	Distance of movement of inclining weights (inches)
GM	Metacentric height (inches)
M_v	Virtual mass
Q	Pumping rate (gallons/min)
S	Projected area of fin (sq. ft.)
s	Projected area of fin (sq. in.)
s'	Projected area of fin over which boundary layer control is applied (sq. in.)
V	Speed (knots)
v	Speed (ft./sec.)
w	Inclining weight (pounds)
α	Effective angle of attack
α_i	Induced angle of attack for aspect ratios less than infinite
α_o	Angle of attack for infinite aspect ratio
$\triangle$	Displacement (pounds)
θ	Angle of heel (degrees)
λ	Linear Scale factor

Symbol	Meaning
ρ	Mass density ($\frac{\text{lb. sec.}^2}{\text{ft.}^4}$)
τ	Induction constant

Subscripts

s	Full scale ship
m	Model

I. INTRODUCTION

Ship stabilization systems employing fins have become increasingly numerous in recent years, and an abundance of literature is available attesting to their satisfactory performance [1],[2],[3]. However, model testing of fin stabilization systems has been extremely limited, principally because of lack of facilities for model testing in sea-keeping basins. Instrumentation is presently available to perform model testing of fin stabilization systems, and adequate facilities for performing such testing will soon be available.

Model testing in general requires equivalency between model and ship Froude numbers. This results in Reynolds numbers appreciably lower for model than for ship, and leads to "scale effect" when dealing with fins or other lift producing devices. Basically, "scale effect" is the reduction of maximum obtainable lift coefficient and reduction of the angle of attack at which this maximum lift coefficient occurs for any given airfoil as Reynolds number is decreased. For the Reynolds numbers normally encountered in model testing, the boundary layer for a geometrically similar fin would be laminar, and laminar separation would occur for very small angles of attack. From data contained in reference (4), it is anticipated that the maximum lift coefficient obtainable for such a fin would approach that for a flat plate, or $C_L(\max) = 0.8$.

Because of these "scale effects", no direct correlation can be obtained between the dynamic effects of geometrically similar model stabilization fins and full scale stabilization fins. This lack of correlation has been recognized[5], but to date no published data is known to be available for solving this basic problem as it applies to ship model testing.

It is the proposal of this thesis that direct correlation between model and ship fin angle of breakdown and total lift (or inclining moment) can be obtained. Two separate and essentially unrelated methods of attack will be investigated. In the first method, it is proposed to disregard geometrical similarity between ship and model fin dimensions, and investigate the effect of varying model fin area and aspect ratio on total lift, maintaining equivalency in model and ship fin angle of breakdown. In the second method, a geometrically similar fin constructed of perforated sheet for its lifting surface and employing boundary layer control will be used. This fin will be used to investigate the effect of boundary layer control suction or pumping rate on the total lift and angle of breakdown of the geometrically similar fin. Results from these investigations will be compared with the anticipated total lift or inclining moment to be obtained from the full scale ship fin and the geometrically similar model fin without boundary layer control.

All fins to be tested will be mounted on a model of a DD445 Class destroyer (scale factor $\lambda = 67.09$) and tests will be made in the M.I.T. Ship Model Towing Tank. Based on information contained in references (6) and (7), a ship speed of 15 knots is considered typical for the design of ship roll stabilization fins. For equivalency of Froude numbers between ship and model, tests will be conducted at a model speed of 1.829 knots.

II. PROCEDURE

A. Development of the low aspect ratio fin

Based on the results contained in reference (4), a curve of fin angle of breakdown as a function of effective Reynolds number was plotted. The effect of induced angle of attack as a function of aspect ratio was calculated following the procedures outlined in references (8) and (9), and additional curves of fin angle of breakdown as a function of both Reynolds number and aspect ratio were plotted (see Figure I).

The inclining moment for both ship and model fin is a function of the product of lift coefficient and fin area. Because of the reduction in maximum lift coefficient obtainable from the model fin caused by "scale effect", it was decided to maintain equivalency between the product of lift coefficient and fin area for ship and model. Based on an anticipated maximum lift coefficient for the ship fin of 1.35, a typical ship fin area of 50 square feet (10 ft. span and 5 ft. chord) and an anticipated maximum lift coefficient for the model fin of 0.72, a required fin area of 3 square inches was calculated.

This model fin area of 3 square inches was maintained constant while varying the fin aspect ratio, and the Reynolds number based on fin chord length and a model speed of 1.829 knots was calculated for each aspect ratio. These points were also plotted on the curves of Figure I.

By comparing this latter curve with the original curves, it was determined that a model fin having an aspect ratio of 7/16 geometric (assumed to be 7/8 effective because of the end plate effect of the skin of the model) would have the same angle of breakdown (24 degrees)

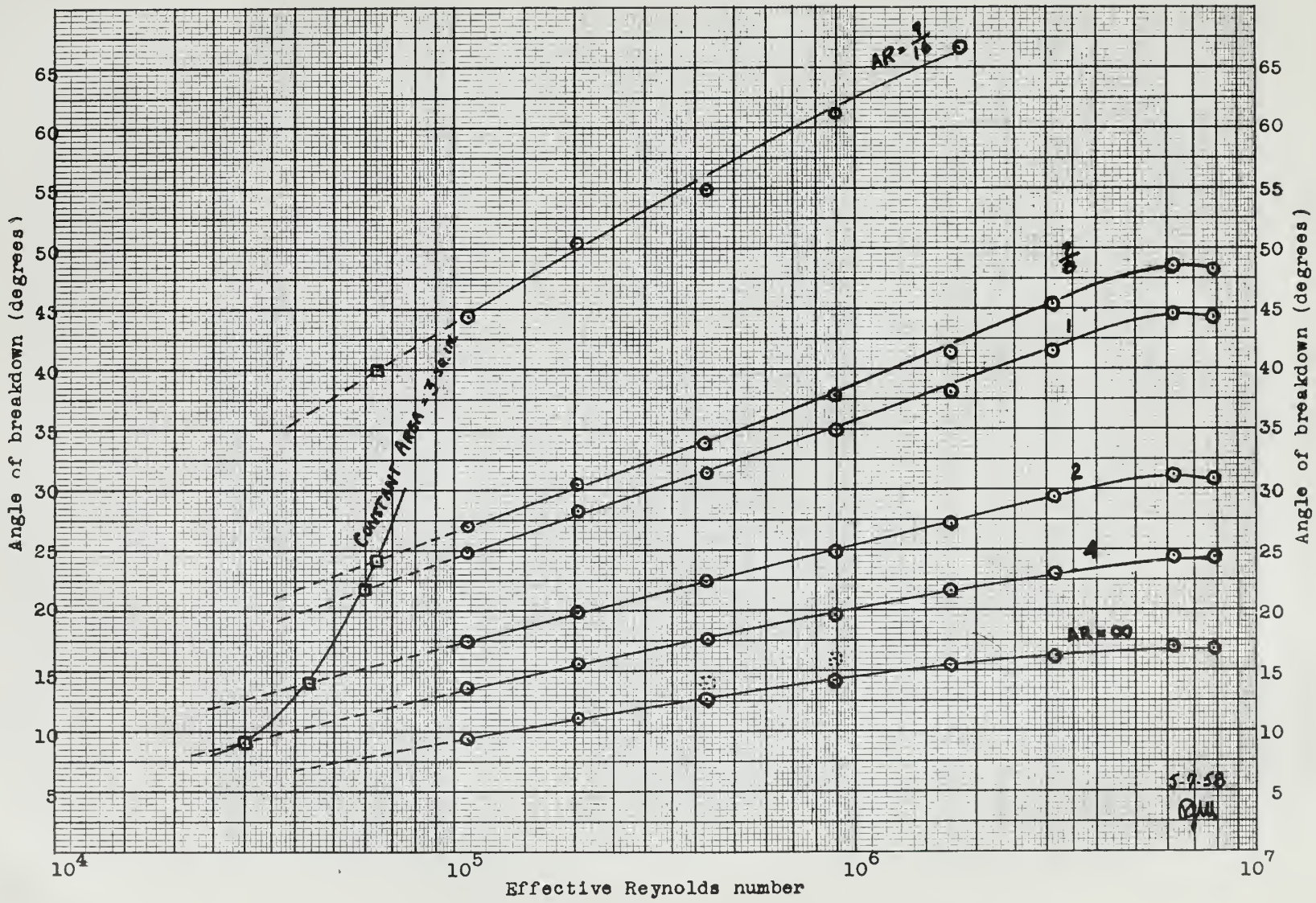

FIGURE I

Curves of angle of breakdown for various aspect ratio NACA airfoils as a function of Reynolds number

as the previously selected typical ship fin having an effective aspect ratio of 4. A model fin with an NACA 0018 airfoil section meeting these specifications was manufactured from solid brass stock for use in the model tests.

B. The geometrically similar fin

The principal difficulty presented by the use of boundary layer control with the geometrically similar fin was the determination of the correct pumping rate to be used to obtain the desired lift and angle of breakdown. Schrenk and Ackeret discuss the use of boundary layer control for obtaining increased angles of stall in aircraft, but their work was done at much higher Reynolds numbers than will be encountered in ship model tests. Many of their papers have been translated from the original German and appear in NACA Technical Memorandums. Boundary layer control by suction is also discussed quite thoroughly in Chapter XIII of reference (10), and the same principles are used in demonstration models of airfoil sections in which smoke jets are used to represent streamlines.

After discussing the problem with several members of the faculty, it was concluded that the best procedure would involve an experimental determination of pumping rate. Therefore, it was decided to make several series of runs at various pumping rates to determine what pumping rate, if any, would produce the desired results.

The manufacture of the geometrically similar fins is described in Appendix A.

C. Procedure for recording and evaluating data

Appendix A gives a thorough description of the equipment used in the experimental work. This section will describe the methods used in applying this equipment.

Since the Sanborn Recorder used for this thesis was also being used for other thesis work, it was necessary to recalibrate the recorder and Autosyn before each series of runs. For this calibration, the model was placed on the tilting table so that the model could be inclined in roll. Readings were taken on the recorder for every 1/2 degree of inclination up to a maximum of $6\frac{1}{2}$ degrees. The model was returned to zero roll angle between each reading. The Autosyn was oriented to give readings in its linear range over the range of roll angles anticipated for the runs. The recorder was adjusted to give approximately 1 cm. deflection for each degree of Autosyn deflection. A curve of recorder deflection as a function of roll angle was plotted for use in later interpretation of data.

In weighing the model, the 400 cycle and 60 cycle power cables were attached to the model. In addition, when weighing the model prior to making runs with the geosim fin employing boundary layer control, the fins, tubing, pump, and pump suction hoses were filled with water.

The model was then placed in the tank and connected to the towing and supporting cables. The power cables were connected to the model and the ballasting weights were adjusted to give a zero angle of heel on the previously calibrated recorder. When adjusting for zero angle of heel for the boundary layer control runs, the adjustment was made with the pump running at the desired pumping rate. This corrected for the effect of the pump motor torque and pump discharge jet.

The model metacentric height (GM) was determined by an inclining experiment. With the model connected to the towing and supporting cables and the power cables connected to the model and energized, two inclining weights (totaling 0.2045 pounds) were moved 2.5 inches to

starboard and the resultant angle of heel measured on the Sanborn Recorder. This was done twice to insure consistent results.

On completion of the inclining experiment, the model was ready for a series of runs for a given fin (and given pumping rate for those runs employing boundary layer control). All runs for a given condition were made without interruption to eliminate fluctuations in equipment parameters.

Because of the varying friction from the two additional supporting cables, it was impractical to maintain constant model speed throughout a given run with the installed equipment at the M.I.T. Towing Tank. Since this varying friction was a function of the distance down the tank, it was decided to give the model an initial acceleration to a speed slightly higher than the desired speed of 1.829 knots. In so doing, the model would slow to a speed slightly lower than the desired speed in the center of the tank, and then reaccelerate to a final speed slightly higher than the desired speed at the end of the tank. Only the latter portion of each run, during which the model speed was the desired speed of 1.829 knots, was considered for recording purposes.

To insure that consistent data was obtained, an average of four runs were made for each fin angle used. During interpretation of the data, in cases where the recorded speed did not coincide with the desired speed of 1.829 knots, the recorded angle of roll was corrected for this speed variation. Since induced angle of roll varies directly with the lift produced by the fin, and this in turn is a function of the square of the speed, the correction applied to the recorded angle of roll was the ratio $\left(\frac{1.829}{V_m}\right)^2$. In no case did this correction amount to more than 3% of the recorded value.

Since the drag force produced by the fins is a function of fin

angle of attack, it was necessary to readjust the speed weights and accelerating distance for each fin angle and fin condition. Typical values for the four series of runs are listed in Appendix B.

III. RESULTS

A. The low aspect ratio fin

Curve I of Figure II is a plot of the observed inclining moment developed as a function of fin angle of attack for the low aspect ratio fin used in the experimental work.

Curve II of Figure II is a plot of the anticipated inclining moment as a function of fin angle of attack for a typical prototype ship fin as developed in Part E of Appendix B.

B. The geometrically similar fin

Figure III contains plots of the observed inclining moment developed as a function of fin angle of attack for the geometrically similar fin under the following conditions:

Curve	Condition
I	All holes sealed and no boundary layer control applied
II	Boundary layer control applied to the low pressure surface, pumping rate of 0.75 GPM ($C_q = 0.0725$)
III	Boundary layer control applied to the low pressure surface, pumping rate of 1.5 GPM ($C_q = 0.145$)

Curve IV of Figure III is a plot of the anticipated inclining moment as a function of fin angle of attack for a typical prototype ship fin as developed in Part E of Appendix B.

FIGURE II

Inclining moment developed by the low aspect ratio fins as a function of angle of attack

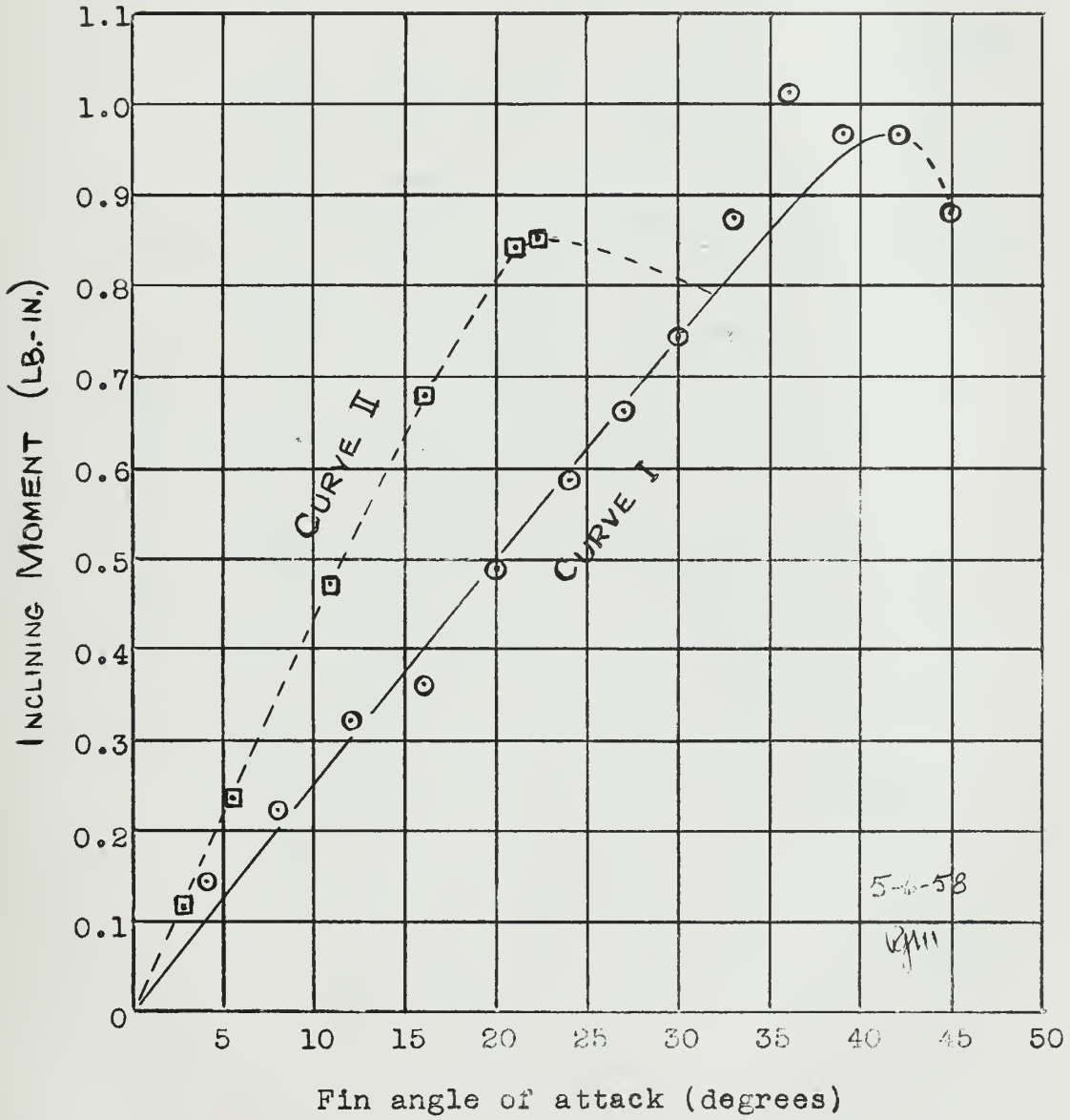

Key

⊙———low aspect ratio fin

⊡- - - - typical prototype ship fin

FIGURE III

Inclining moment developed by the geometrically similar fins as a function of angle of attack

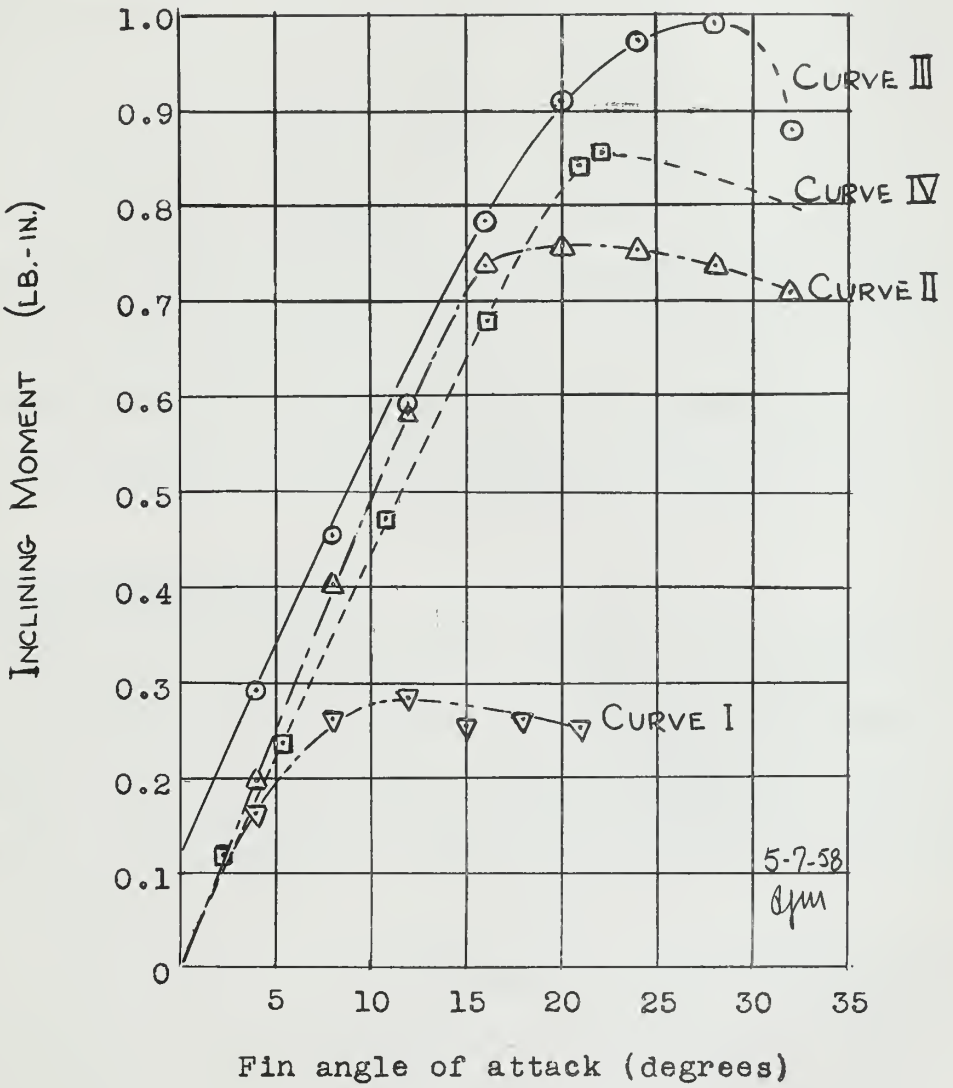

Key

▽——--——▽ without boundary layer control

△——-——△ boundary layer control applied, pumping rate of 0.75 GPM

⊙————⊙ boundary layer control applied, pumping rate of 1.5 GPM

⊡-----⊡ typical prototype ship fin

IV. DISCUSSION OF RESULTS

A. The scaled down anticipated prototype inclining moment curve

For purposes of comparing the experimental results of this thesis and the corresponding information from the full scale ship, a plot of anticipated inclining moment as a function of fin angle of attack for the prototype ship fin was developed. The details of the procedure for this development are contained in Part E of Appendix B. It must be noted that to the best knowledge of the authors, actual values as would be measured on existing fin stabilization systems already installed in ships have not been published. However, it is the authors' belief that the values developed in accordance with the references indicated in the Appendix are reasonable and can be considered as representing the typical case.

B. The low aspect ratio fin

As can be seen in Figure II, the low aspect ratio fin developed a maximum inclining moment of 0.966 lb.-in. at an angle of breakdown of 41 degrees, while the scaled down anticipated prototype fin developed a maximum inclining moment of 0.854 lb.-in. at an angle of breakdown of 22.1 degrees.

The method used to select the dimensions of the low aspect ratio fin is described in Part A of Appendix A. There were two basic errors in this original procedure. The first error was the assumption that the effective aspect ratio of the fin would be twice the geometric aspect ratio because of the proximity of the hull (end plate effect). Figure IX shows the large gap between the low aspect ratio fin and the model hull at a relatively high angle of attack. The effect of this gap would be noticeable at both moderate and high angles of attack, and

it is doubtful that the proximity of the hull afforded any increase in effective aspect ratio for this fin. It must be noted, however, that the angle of breakdown for a fin having an aspect ratio of 7/16 (the geometric aspect ratio of the fin tested) at the Reynolds number corresponding to a model speed of 1.829 knots is 40 degrees, as obtained from Figure I. This agrees very favorably with the observed value of 41 degrees.

The second error committed was the assumption that the prototype ship fin would have a $C_L(max) = 1.35$ at a ship speed of 15 knots. As explained in Part E of Appendix B, a value of $C_L(max) = 1.0$ is considered to be more reasonable.

The actual value of $C_L(max)$ developed from the low aspect ratio fin is calculated in Part F of Appendix B, and was 0.654. The value assumed in Part A of Appendix A when selecting the dimensions for this fin was $C_L(max) = 0.72$. The calculated value is considered reasonable and representative for such fins, and within the limits of experimental accuracy.

In Part F of Appendix B the dimensions of a low aspect ratio fin which would produce the same inclining moment (0.854 lb.-in.) and angle of breakdown (22 degrees) as the scaled down prototype were developed. These calculations give a fin with a geometric aspect ratio of 7/8 and an area of 2.57 sq. in. This area is 1.63 times the area of a geometrically similar fin, and the relative virtual mass effect of this fin will be 2.26 times the virtual mass effect of the geometrically similar fin. Calculations for virtual mass effect are contained in Part G. of Appendix B.

C. <u>The geometrically similar fin</u>

Figure III shows the results of experimental work with the

geometrically similar fin under various conditions of boundary layer control. A plot of the scaled down anticipated inclining moment from the prototype ship fin is included for purposes of comparison.

The angle of breakdown for the geometrically similar fin without boundary layer control was observed to be 12 degrees. This is in close agreement with the angle of breakdown predicted from Figure I (11.5 degrees) for an airfoil having an aspect ratio of 2 and Reynolds number of 2.18×10^4. A calculation of the value of $C_L(max)$ developed by this fin in this condition gave a value of only 0.342. The validity of these results is questionable because of the boundary layer phenomena at these low values of Reynolds number.

Inspection of curve III of Figure III reveals that with a boundary layer control pumping rate of 1.5 GPM, some lift was probably developed at zero angle of attack. It should be pointed out that this lift was only developed in conjunction with the forward motion of the model, since the model was trimmed and the instrumentation calibrated to give zero angle of heel using this pumping rate with the model at rest. It is also noted that the maximum inclining moment developed by the geometrically similar fin under this condition of boundary layer control (0.983 lb.-in.) also exceeded the maximum scaled down inclining moment of the prototype ship fin. On this basis, a boundary layer control pumping rate of 1.5 GPM is considered excessive.

Curve II of Figure III shows the inclining moment developed by the geometrically similar fin with a boundary layer control pumping rate of 0.75 GPM. This curve is below the scaled down inclining moment curve for the prototype fin. It is the contention of the authors that at some boundary layer control pumping rate between the values of 0.75 GPM and 1.5 GPM, the geometrically similar fin will produce the same inclining

moment curve as the scaled down inclining moment curve for the prototype ship fin. The exact value of boundary layer control pumping rate to be applied can only be developed by further experimentation, but it would appear reasonable that a value between 0.90 GPM and 1.10 GPM should produce the desired effect.

To provide for correlation of the experimental results obtained in this thesis with boundary layer control experimental work under different conditions of fin size and model speed, a dimensionless pumping rate coefficient C_q was developed in Part H of Appendix B. Applying this coefficient to the values of pumping rate used in this thesis, for the 1.5 GPM pumping rate, $C_q = 0.145$, and for the 0.75 GPM pumping rate, $C_q = 0.0725$.

Because of the many difficulties encountered in adapting the instrumentation of the M.I.T. Towing Tank to conform with the requirements of this thesis, the time available for experimental work was limited. In addition to investigating the effect of varying boundary layer control pumping rate between the values actually tested, it was also proposed to investigate the effect of changing the location of the area of the fin to which boundary layer control was applied. Since laminar separation occurs near the region of minimum pressure and progresses toward the leading edge as angle of attack is increased, the authors intended to investigate the effect of boundary layer control applied only to the leading 25% of the low pressure surface. An additional area of investigation would be the effect of applying boundary layer control to both the low and high pressure surfaces.

Since the stabilization fins actually used on ships are usually of the doubly all-moveable type, the effect of boundary layer control on a geometrically similar model of a doubly all-moveable fin should also be

investigated. Such experimental investigations in the M.I.T. Towing Tank would be difficult because of the small dimensions of any practical geometrically similar fin. This would complicate the manufacture of doubly all-moveable fins to model scale, and would also present additional installation problems. However, it is felt that the problems presented are not insurmountable. In particular, once the principles for application of boundary layer control to simple fins have been developed, they should be applicable to a doubly all-moveable fin with little or no modification.

The effectiveness of the proximity of the model hull in doubling the aspect ratio of the fin is subject to some question. As installed in the model, both the low aspect ratio fins and the geometrically similar fins used in the experimental work had a gap of 0.16 inches between the hull and the root of the fin. Reference (6) assumes that the effect of the hull increases aspect ratio by a factor of 1.7, and assigns a factor of 1.4 to the effect produced by an end plate. Experimental work with model fins employing end plates and with no gap between the fin root and the hull is another area that can be investigated.

With reference to the instrumentation used in this thesis, there are several recommendations that should be made. The boundary layer control pump discharge should be led aft on the model and discharged astern, rather than over the side of the model. This would eliminate the need for calibrating the instrumentation in the model to take the jet effect of the pump discharge into account. Although no difficulty was experienced in obtaining the proper ballasted condition for the model with the 4.5 GPM pump used, a smaller pump having a lower capacity would be just as satisfactory and would be beneficial in cases where space and weight were critical in the model. In addition, a smaller pump could probably be mounted in the model with its motor axis athwartships rather than

fore and aft, thus eliminating any effect of motor torque on the heel angle of the model.

D. General towing tank procedure

The Autosyn unit with its attached pendulum used for measurement of model heel angle gave satisfactory results, as evidenced by the consistency of results obtained between the various runs made at any given fin condition. The gyro unit available at the M.I.T. Towing Tank was not used because of the added complexity it would have added to the model instrumentation, both from power and space and weight considerations. The authors feel that the ideal instrumentation for measurement of model heel angle would be a Microsyn with a damped pendulous unit attached. Unfortunately, one was not available for use at the time the experimental work was conducted.

Since it was impractical to maintain a constant model speed in the M.I.T. Towing Tank as finally adapted for use, considerable time was consumed in adjusting the dynamometer weights and accelerating distances to obtain the speed variation desired. The experimental work would have been greatly simplified if a towing carriage had been available. A carriage with a rigid connection to the model towing bracket connection would have eliminated this speed variation and the tendency of the model to veer to the side of the towing tank when a heel angle was produced by the fins.

For future experimental work of this nature at the M.I.T. Towing Tank, an additional supporting cable should be strung at the same height as the upper supporting cable used during this thesis, but on the opposite side of the towing cables. This would provide additional support to the towing bracket and result in a further reduction of the tendency of the model to veer toward the side of the towing tank when

a heel angle is produced by the fins. It should be noted that the end result of these additional supporting cables is an attempt to produce a "rigid" monorail, such as would exist with a towing carriage.

V. CONCLUSIONS

1. It is feasible to obtain equivalency of scaled down inclining moment and angle of breakdown between model and ship by reducing the aspect ratio of the model fin and increasing its area. However, this results in a greatly increased virtual mass effect as compared with a geometrically similar fin. This increase in virtual mass effect is not desired in experiments designed to measure the effectiveness of fins in reducing roll.
2. It is also feasible to obtain equivalency of scaled down inclining moment and angle of breakdown between model and ship by using geometrically similar fins employing boundary layer control by suction.
3. For the specific model conditions of this thesis, a pumping rate coefficient C_q between 0.087 and 0.106, corresponding to pumping rates of 0.90 and 1.10 GPM respectively, should produce the desired equivalency. The exact value of C_q can best be determined experimentally.

VI. RECOMMENDATIONS

1. As a means of obtaining equivalency of scaled down inclining moment and angle of breakdown between ship prototype fin and model fin, a geometrically similar fin employing boundary layer control is preferable to a fin of reduced aspect ratio and increased area.
2. The principles used and the results obtained should be investigated in regard to their application to model tests involving other fin shapes and uses, such as anti-pitching fins and rudders.
3. Future investigations in boundary layer control should include the effect of varying the location of the area of the fin surface to which boundary layer control is applied, the effect of varying the pumping rate, and the effect of applying boundary layer control to both high and low pressure surfaces of the fin.
4. Once boundary layer control procedures and methods have been developed for the simple fin, similar principles should be applied to the development of corresponding procedures for the doubly all-moveable fin.
5. The effect of boundary layer control on drag should be investigated.
6. Experimental work should be carried out to determine the effect of end plates on fins and the effect of filling in the gap between the model hull and the root of the fin.
7. In cases where weight and space are critical, a pump having a smaller capacity than the 4.5 GPM pump used could be advantageous.
8. The overboard discharge for the pump should be led astern rather than over the side.
9. A Microsyn unit with an attached damped pendulous unit would be preferable to the Autosyn used for measuring model heel angle.

10. A towing carriage rather than the towing cables would permit model speeds to be maintained at a constant value, and would eliminate the tendency of the model to veer toward the side of the tank when a heel angle was developed by the fins.

11. For future experimental work of this nature at the M.I.T. Towing Tank, an additional supporting cable should be strung at the same height as the upper supporting cable used during this thesis but on the opposite side of the towing cables.

VII. APPENDIX

APPENDIX A

DETAILS OF PROCEDURE

A. Development of the low aspect ratio fin

Table I lists maximum lift coefficient $C_L(max)$ and angle of breakdown α_o for an infinite aspect ratio airfoil having an NACA 0018 section as a function of effective Reynolds number. Values were obtained from reference (4).

TABLE I

NACA 0018 Airfoil Data

Effective Reynolds No.	$C_L(max)$	α_o (degrees)
7.84×10^6	1.43	16.8
6.24 "	1.44	17.0
3.30 "	1.33	16.2
1.73 "	1.18	15.5
0.866 "	1.08	16.0
0.430 "	0.97	14.0
0.214 "	0.90	11.0
0.109 "	0.80	9.5

To correct for the induced angle of attack for rectangular wings having aspect ratios not equal to infinity, the procedure outlined in references (8) and (9) was followed, using the formula $\alpha = \alpha_o + \alpha_i$, where $\alpha_i = \frac{C_L}{\pi AR}(1 + \tau)$. For computing angles of breakdown, this becomes $\alpha_i = \frac{C_L(max)}{\pi AR}(1 + \tau)$. Values of τ applied are obtained as a function of aspect ratio from graphs in references (8) and (9). These graphs represent the results of Glauert's lifting line theory, and as such, are not truly correct in light of later circulation theory. However, lacking any finer corrections, these graphs will be used, and the values of τ used are listed in Table II.

TABLE II

Values of τ as a function of Aspect Ratio

Aspect Ratio	4	2	1	7/8	7/16
τ	0.125	0.08	0.054	0.051	0.042

Table III lists the results of these calculations, showing the anticipated angle of breakdown for low aspect ratio airfoils as a function of Reynolds number.

TABLE III

Airfoil angle of breakdown vs. Aspect Ratio and effective Reynolds No.

Effective Reynolds No.	α_o (degrees)	Aspect Ratio →	4	2	1	7/8	7/16
7.84×10^6	16.8	α ↓	24.1	30.9	44.2	48.1	79.0
6.24 "	17.0		24.4	31.2	44.6	48.6	79.6
3.30 "	16.2		23.0	29.3	41.7	45.3	74.1
1.73 "	15.5		21.6	27.1	38.1	41.3	66.8
0.866 "	16.0		19.7	24.8	34.9	37.9	61.2
0.430 "	14.0		17.7	22.2	31.3	33.9	54.9
0.214 "	11.0		15.6	19.8	28.3	30.7	50.4
0.109 "	9.5		13.6	17.4	24.9	27.0	44.3

It will be noted that the values of α_o for the NACA 0018 airfoil at Reynolds numbers of 0.866×10^6 and 0.430×10^6 are considerably higher than the faired curve values. As discussed in reference (4), this is caused by the critical range of Reynolds numbers for this airfoil. Within this critical range the boundary layer is undergoing transition from laminar flow to turbulent flow, and as the transition point moves toward the leading edge with increasing Reynolds numbers, it approaches the separation point, reducing the region of separated flow over the airfoil. This tends to increase the maximum lift coefficient obtainable as well as the angle at which it occurs. Since the range of Reynolds numbers for this investigation is either well above or well below this

critical transition region, these two points will be disregarded. As an aid to plotting the curves for lower aspect ratios, the faired values of α_o at these two Reynolds numbers will be used in the calculations. The values listed in Table III for these two Reynolds numbers were obtained in this manner.

Rather than select one particular ship stabilization fin from the many in current use as a prototype, a study of reference (7) and plans of the stabilization fin installed on the U.S.S. GYATT revealed that a typical ship fin would have a 10 ft. span and 5 ft. chord (aspect ratio of 2 geometric or 4 effective) with a symmetrical airfoil section similar to the NACA 0018 airfoil. It was further decided to limit the scope of the thesis to an investigation of fin phenomena at a ship speed of 15 knots. Based on these characteristics, the following data was obtained for the ship fin.

Reynolds No. (at 59° F. in salt water)	9.89×10^6
Fin angle of breakdown	Approx. 24 degrees
Maximum section lift coefficient	Approx. 1.5

According to reference (4), $C_L(max)$ will be a function of wing planform loading, and for initial calculations, a value of 0.9 $c_\ell(max)$ will be assumed for the rectangular fin used.

$$C_L(max) = 0.9 \times 1.5 = 1.35$$

The following equations represent fin stabilization on the ship and on the model, respectively.

$$\Delta_s \left(GM_s \sin \theta + k \frac{BM_s}{100} \right) = 2 \left(\frac{\rho}{2} C_L S_s v_s^2 \right) x \text{ lever}_s$$

$$\frac{\Delta_s}{\lambda^3} \left(\frac{GM_s}{\lambda} \sin \theta + k \frac{BM_s}{100\lambda} \right) = 2 \left(\frac{\rho}{2} C_L \frac{S_s}{\lambda^2} \frac{v_s^2}{\lambda} \right) x \frac{\text{lever}_s}{\lambda}$$

The value of C_L on the model fin will be lower than C_L on the ship fin because of "scale effect." If geometric similitude is maintained on all other factors of the above equations, then in order to develop the same angle of roll on ship and model, the product of fin lift coefficient and fin area must be maintained proportional between ship and model, the constant of proportionality being λ^2. For the values of Reynolds numbers encountered with the model fin, reference (4) states that the maximum sectional lift coefficient approaches that for a flat plate, or $c_\ell(\max) = 0.8$. Assuming, as for the ship fin, that $C_L(\max)$ for a rectangular airfoil is 0.9 x $c_\ell(\max)$, the value obtained for the model fin is

$$C_L(\max) = 0.9 \times 0.8 = 0.72$$

Then

$$\left[C_L(\max) \times S\right]_{model} = \frac{\left[C_L(\max) \times S\right]_{ship}}{\lambda^2} = \frac{1.35 \times 5 \times 10 \times 144}{(67.09)^2}$$

$$= 2.16 \text{ sq. in.}$$

$$S_m = \frac{2.16}{0.72} = 3.0 \text{ sq. in.}$$

This area will be maintained constant, and a cross plot developed of model fin Reynolds number as a function of effective aspect ratio. Points so determined are plotted on the curves previously developed in Figure I. Table IV lists the values obtained in the manner.

TABLE IV

Model fin Reynolds No. vs. Aspect Ratio

Fin area (sq. in.)	Geom. AR	Effective AR	Span (in.)	Chord (in.)	Reynolds No.(at 70° F. in fresh water)
3.0	2	4	2.45	1.225	2.99×10^4
↓	1	2	1.732	1.732	4.23 "
	1/2	1	1.225	2.45	5.98 "
	7/16	7/8	1.145	2.62	6.4 "

From the curves of Figure I, it is noted that the low aspect ratio fin with an effective aspect ratio of 7/8 should have the same angle of breakdown as the ship fin, approximately 24 degrees. Since the area of the model fin has already been calculated to maintain equivalency of total lift developed by ship and model fins, this fin should meet the requirements of the thesis proposal.

B. Fin manufacture and installation

The low aspect ratio fins were manufactured from solid brass bar stock to conform with the section shape for the NACA 0018 airfoil. As developed in the preceeding paragraphs, the fins had a projected area of 3 square inches, with a span of 2.62 inches and a chord of 1.145 inches. The fin shafts were made of 1/4 in. brass tubing and were located a distance of one third of the chord length from the leading edge. These fins were installed as close as possible to the skin of the model without interfering with their angular movement. This resulted in a gap of 0.16 inches between the root of the fin and the model, measured at the shaft centerline. As can be seen in Figure IX, the low aspect ratio fin will have a large gap between it and the model at large angles of attack.

The construction of the geometrically similar fin is shown in Figure IV. The end pieces were manufactured from solid brass bar stock to conform with the section shape for the NACA 0018 airfoil. However, all dimensions were reduced by 0.02 in. to allow for the thickness of the perforated brass sheet which formed the surface of these fins. The geometrically similar fins had a projected area of 1.58 square inches, with a span of 1.789 inches and a chord of 0.894 in.

The brass sheeting was perforated with 24 staggered rows of holes per inch along the span of the fin. The holes in each row were 0.023 in. in diameter and were spaced to provide 18 holes per inch along the chord

of the fin. The end pieces in the fin sealed off the holes for a distance of 0.118 in. at the root and the tip of the fin. The trailing edge of the fin was sealed off for a distance of 0.197 in. (22% of the chord) where the upper and lower surfaces were soldered together. The fin shafts were made of 1/4 in. brass tubing as with the low aspect ratio fins, and were similarly located.

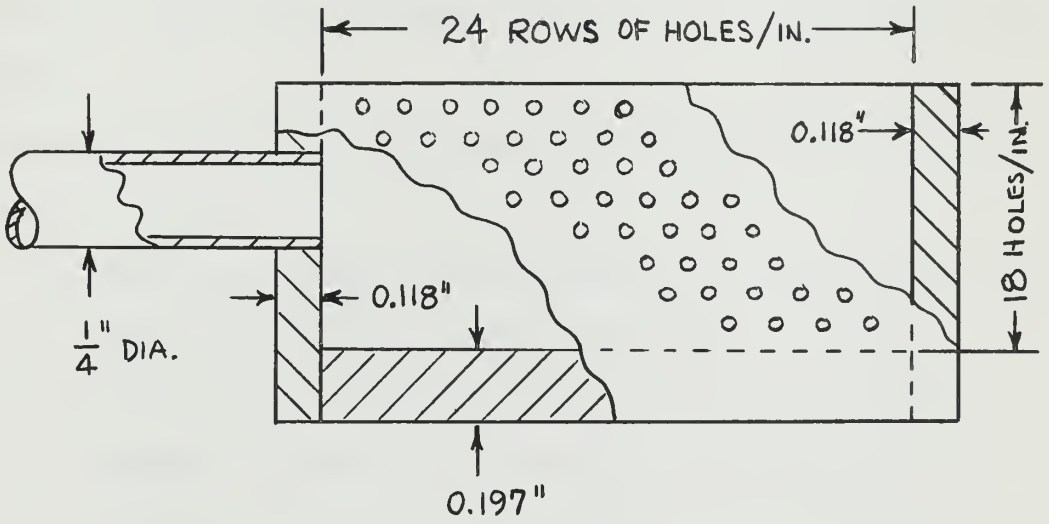

FIGURE IV. Sketch showing construction of geometrically similar fin.

Figure X shows the geometrically similar fin in position on the model. The gap between the root of the fin and the model is 0.16 in., measured at the shaft centerline. In use, for those runs employing boundary layer control, the holes in the high pressure surface of each fin were sealed with a mixture of parafin and beeswax. The holes in the low pressure surface of the fins were left open from the leading edge to the portion of the trailing edge that had been sealed during manufacture. For those runs in which boundary layer control was not used, all holes in both surfaces of the fins were sealed.

Figure V shows the boundary layer control pump connections to the inboard end of the geometrically similar fin shafts. The discharge from

the pump was piped overboard through 1/2 inch rubber tubing. A clamp on the rubber tubing permitted the pumping rate to be regulated.

C. Details of the model instrumentation

The model used for this thesis was M.I.T. model No. 18 (ETT model No. 395). It is a model of the DD445 Class destroyer, built to a scale factor of 67.09. Body plans to the scale of the model are available in the M.I.T. Towing Tank files. Figure V shows an interior view of the model with the towing bracket removed. Figure VI shows the model in the Towing Tank.

Referring to Figure V, the following items were installed in the model:

1. The Autosyn synchro with the pendulum attached to its shaft. This unit was used to obtain the heel angle information resulting from the developed fin inclining moment. The shaft axis of the Autosyn was placed at a height above the keel corresponding to the calculated center of roll for the model. The shaft axis is in the centerline plane and is parallel to the base line.
2. The towing bracket pivot. This pivot provides freedom of movement about both the roll and pitch axes for the model. The pivot is located at the midship section of the model, with its roll axis at a height above the keel corresponding to the center of roll, in the centerline plane and parallel to the base line.
3. The fins and fin shaft bushings. The fin shaft bushings were manufactured to provide a close fitting bearing surface for the fin shafts that would be watertight and yet permit rotation of the fin shafts in the bushing. The

centerline axis of the fin shafts were located so that the fins would coincide with the bilge keel location at the skin of the ship and the shaft centerlines (extended) would intersect at the height of the center of roll. The fins are located at Station 11 of the model, which provides the maximum lever arm for this model. A pointer is attached to each fin shaft, and fin angle of attack with respect to the base line can be read from protractors attached to the fin shaft bushings.

4. The boundary layer control suction pump. The pump used was an Eastern Industries Model A-1 pump, obtained from Central Scientific Company (Catalog No. 17955). It has a maximum pumping capacity of 4.5 GPM and is driven by a 115 volt A.C.-D.C. motor. The dimensions of the pump-motor unit are 2 3/4 inches in diameter and 7 1/4 inches long, and the unit weighs 3 1/2 pounds.

The center of roll for the model was calculated for a condition of loading that would correspond to the 12.45 ft. waterline for the prototype ship, with a desired GM of 2.80 feet. This corresponds to a GM of 0.5 in. on the model and a model weight of 18.25 pounds. Reference (7) states that the center of roll is assumed to be midway between the center of gravity and the center of buoyancy. Based on these considerations, the assumed center of roll for the model is 2.14 inches above the base line.

D. Details of the towing tank procedure.

The general operating procedures for the M.I.T. Towing Tank are contained in reference (11). Unfortunately, the lack of a carriage at the Towing Tank makes any experimental work in which information from instrumentation in the model is to be transmitted to recorders rather

difficult. Additional difficulties are presented when model roll or heel angle information is desired because of the tendency of the model to veer toward the side of the towing tank.

The instrumentation contained in the model was discussed in the preceeding paragraphs. Power to the Autosyn and pump motor was led to the model by means of a "fishing pole" arrangement consisting of an aluminum U-channel and two cables. This can be seen in Figure VI. A five-conductor cable carried 400 cycle power to the Autosyn rotor and from the Autosyn stator to a bridge rectifier. A schematic wiring diagram for this 400 cycle power distribution is given in Figure XI. The 400 cycle power supply is described in reference (12). The second cable supplied 115 volts, 60 cycle power to the pump motor. A switch in this cable, located on the "fishing pole", permitted the motor to be turned on and off from this remote position.

During a run, one man was required to walk along with the model, carrying the "fishing pole". It is imperative that this be done in such a manner that the cables from the "fishing pole" to the model do not cause a false roll or heel angle to be induced, and model speed must not be influenced. With practice, it was possible to eliminate any influence on the model from the power cables.

A second man operated the model towing dynamometer, recorded speeds as read from the Eput meter on a wire recorder, and operated the Sanborn recorder, pressing the "marker" button simultaneously with recording each speed reading. On completion of each run, the speed recordings from the wire recorder were played back and transcribed onto the Sanborn Recorder tape under the corresponding marks.

Since the Sanborn Recorder used had a D.C. amplifier, the 400 cycle output from the Autosyn stator had to be rectified. As indicated in the

wiring diagram of Figure XI, a bridge rectifier was used, and the D.C. output of the rectifier was connected to the input of the recorder amplifier through a three-conductor jack. The cart containing the 400 cycle power supply, rectifier, and Sanborn Recorder is shown in Figure VII.

Considerable difficulty was experienced in early attempts to keep the model centered in the towing tank and directly under the towing cable. Satisfactory runs were obtained only after two additional supporting cables were strung the length of the tank and a rather heavy, rigid towing bracket was fabricated. The supporting cables were 40-lb. test nylon monofilament fishing line. One cable was led down the center of the tank directly under the lower towing cable and six inches above the water level in the tank. This passed through an eye centered in the towing bracket, and the six-inch height just cleared the spray shield at the forward end of the instrumentation compartment on the model. The other cable was offset to the right of the towing cables, but at a height midway between the upper and lower towing cables. This upper, offset cable passed through an eye on the end of a rigid arm connected to the towing bracket. Both of these supporting cables and the towing bracket are visible in Figure VI.

APPENDIX B

SUMMARY OF DATA AND CALCULATIONS

A. The low aspect ratio fin

1. The inclining experiment

Weight moved - 0.2045 lb.

Distance moved - 2.5 in.

Resulting heel angle - 2.75°

Model displacement - 18.25 lb.

$$GM = \frac{w \times d}{\Delta \times \text{Tan } \theta} = \frac{(0.2045)(2.5)}{(18.25)(\text{Tan } 2.75^\circ)}$$

GM = 0.585 in.

2. The runs themselves, the results, and calculated inclining moments.

For convenience in making any future experiments in the M.I.T. Towing Tank, the accelerating weight distance and the difference in weight between the two weight pans are included in these results. These values are listed in Table V.

In calculating inclining moment, the following formula was used:

Inclining moment (in.-lb.) = $\Delta \times GM \times \text{Tan } \theta$

TABLE V

Resistance data, heel angles, and inclining moments for the low aspect ratio fin.

Fin angle (degrees)	Accelerating weight distance (inches)	Weight pan difference (pounds)	Resulting heel angle (degrees)	Inclining moment (inch-pounds)
4	13.0	2.20	0.78	0.145
8	14.5	2.30	1.21	0.222
12	14.0	2.43	1.63	0.322
16	13.0	2.52	1.94	0.362
20	14.0	2.76	2.63	0.490
24	15.0	3.05	3.15	0.586
27	15.0	3.55	3.57	0.664
30	15.0	3.80	4.02	0.747
33	15.0	4.20	4.72	0.878
36	15.0	4.26	5.45	1.013
39	15.0	4.70	5.20	0.966
42	15.0	4.86	5.20	0.966
45	15.0	4.95	4.75	0.883

B. The geometrically similar fin with a pumping rate of 1.5 gallons per minute.

1. The inclining experiment

Resulting heel angle - 2.50°

Calculated GM - 0.644 in.

2. The runs themselves, the results, and calculated inclining moments.

TABLE VI

Resistance data, heel angles, and inclining moments for the geometrically similar fin with a pumping rate of 1.50 GPM

Fin angle (degrees)	Accelerating weight distance (inches)	Weight pan difference (pounds)	Resulting heel angle (degrees)	Inclining moment (inch-pounds)
4	12.5	2.20	1.42	0.291
8	13.5	2.38	2.18	0.456
12	14.5	2.80	2.90	0.594
16	14.4	3.00	3.84	0.784
20	14.0	3.22	4.45	0.910
24	13.2	3.40	4.75	0.972
28	13.0	3.70	4.85	0.992
32	13.0	3.70	4.29	0.879

C. The geometrically similar fin with a pumping rate of 0.75 gallons per minute.

1. The inclining experiment

Resulting heel angle - 2.50°

Calculated GM - 0.644 in.

2. The runs themselves, the results, and calculated inclining moments.

TABLE VII

Resistance data, heel angles, and inclining moments for the geometrically similar fin with a pumping rate of 0.75 GPM

Fin angle (degrees)	Accelerating weight distance (inches)	Weight pan difference (pounds)	Resulting heel angle (degrees)	Inclining moment (inch-pounds)
4	11.5	2.15	0.97	0.199
8	12.5	2.40	1.97	0.403
12	12.7	2.80	2.85	0.584
16	13.0	3.00	3.60	0.738
20	12.0	3.19	3.70	0.759
24	11.2	3.47	3.68	0.755
28	11.5	3.60	3.60	0.738
32	11.5	3.80	3.46	0.710

D. The geometrically similar fin with all holes sealed, no boundary layer control

1. The inclining experiment

Resulting heel angle - 2.35°

Calculated GM - 0.685 in.

2. The runs themselves, the results, and calculated inclining moments.

TABLE VIII

Resistance data, heel angles, and inclining moments for the geometrically similar fins with all holes sealed, no boundary layer control

Fin angle (degrees)	Accelerating weight distance (inches)	Weight pan difference (pounds)	Resulting heel angle (degrees)	Inclining moment (inch-pounds)
4	11.7	1.94	0.75	0.164
8	12.5	2.10	1.20	0.262
12	12.5	2.26	1.30	0.284
15	12.5	2.30	1.19	0.256
18	13.0	2.40	1.20	0.262
21	13.0	2.50	1.155	0.252

E. Calculation of anticipated prototype inclining moment

In making the calculations for the anticipated inclining moment to be obtained from a ship stabilization fin, certain reasonable assumptions were made. The following calculations were based on a simple ship fin having an NACA 0018 airfoil section, a 5 ft. chord and 10 ft. span (geometric aspect ratio of 2, and effective aspect ratio of 4), an average fin submergence of 10 feet and a ship speed of 15 knots.

Reference (4) provides lift curve data for the NACA 0018 airfoil for Reynolds numbers up to 7.84×10^6, but the Reynolds number for a chord length of 5 feet at a ship speed of 15 knots is 9.89×10^6. E. V. Lewis and W. R. Jacobs in reference (13) describe an analytic approach to determining the maximum lift coefficient $C_L(max)$ obtainable under actual ship conditions, taking into account the effect of aspect ratio, surface effect, cavitation, and non-uniform flow around the fin. The end result obtained using this method is a value of $C_L(max) = 1.06$, at a fin angle of attack between 22 and 23 degrees.

J. H. Chadwick, in reference (6), considers a simple fin, such as used in the experimental work of this thesis, operating at a ship speed of 15 knots and fin submergence of 10 feet, to be separation limited.

The value of C_L(max) used in his calculations is 1.0 at a fin angle of 25 degrees (allowing for curvature of the lift curve).

Additional data obtained from the Denny-Brown stabilization fin in reference (2) tends to confirm the above values of C_L(max).

For our purposes of plotting an inclining moment curve for the ship fin, it would seem reasonable that the value of maximum lift coefficient should be in the vicinity of C_L(max) = 1.0, and this value should occur at a fin angle of 22 to 25 degrees. Therefore, the lift curve for the NACA 0018 airfoil at a Reynolds number of 7.84×10^6 will be scaled down to give a value of C_L(max) = 1.0, with the usual correction applied to fin angle for the reduced effective aspect ratio of 4. The resulting calculated inclining moment of the ship fin will be scaled down to model values for purposes of plotting and comparison with model results.

TABLE IX

Development of scaled down inclining moment of ship fins

α_o (Deg.)	C_L	C_L corrected	α_i (Deg.)	α (Deg.)	Lift (lbs.)	Scaled down lift both fins	Scaled down inclining moment(lb.-in.)
2	0.2	0.14	0.72	2.72	4440	0.0294	0.119
4	0.4	0.28	1.44	5.44	8880	0.0588	0.239
8	0.79	0.552	2.83	10.83	17500	0.116	0.471
12	1.14	0.798	4.09	16.09	25300	0.168	0.680
16	1.41	0.986	5.05	21.05	31300	0.207	0.841
17	1.43	1.00	5.12	22.12	31700	0.21	0.854
18	1.28	0.895	4.59	22.59	28400	0.188	0.763

The following equations were used in determining values listed in Table IX:

$$\frac{\alpha_i}{C_L} = \frac{(1+\tau)}{\pi \times AR} \quad \text{in radians, where for AR} = 4, \ \tau \simeq 0.125$$

$$= 5.12 \text{ degrees}$$

$$\text{Lift} = \frac{\rho}{2} C_L \times S \times v^2 = \frac{1.98}{2} \times C_L \times 50 \times (15 \times 1.689)^2$$

$$= 31{,}700 \times C_L$$

$$\text{Scaled down lift} = \frac{\text{Ship fin lift/fin} \times 2 \text{ fins}}{\lambda^3} = \frac{\text{Ship lift}}{151 \times 10^3}$$

Model lever arm: Center of pressure = 0.45 x span for a rectangular airfoil with end plate

Center of pressure = 0.45 x 1.789	= 0.805 in.
Distance from skin to center of roll	3.10 in.
Clearance between fin root and skin	0.158 in.
Total lever arm	4.063 in.

F. Calculation of a recommended low aspect ratio fin

Based on the observed inclining moment for the low aspect ratio fin tested, the following value of $C_L(\max)$ was calculated, using the listed equations.

$$\text{Inclining moment} = 2 \times \text{lever} \times \frac{\rho}{2} \times C_L \times s \times v^2/144$$

$$C_L(\max) = \frac{0.966 \times 144}{1.94 \times 3 \times (3.09)^2 \times 3.84} = 0.654$$

Assuming that this value of $C_L(\max)$ will be obtained by a higher aspect ratio fin, an area for this new fin, referred to in the equations as s(2), was calculated to produce the same inclining moment as the anticipated inclining moment from the prototype fin.

$$s(2) = \frac{s(1) \times \text{lever}(1) \times \text{prototype inclining moment}}{\text{lever}(2) \times \text{inclining moment}(1)}$$

$$s(2) = \frac{3.0 \times 3.84 \times 0.854}{4.0 \times 0.966} = 2.57 \text{ sq. in.}$$

Arbitrarily assigning an aspect ratio of 7/8 to this new fin, its dimensions then become span = 1.50 inches and chord = 1.713 inches. The Reynolds number based on a model speed of 1.829 knots and this chord of 1.713 inches is 4.19×10^4. Checking this against the plot of

Figure I shows that this fin should have an angle of breakdown of 22 degrees.

Measurement of the lever arm for this fin on the body plan of the model gives a lever arm of 4 inches, which checks with the value previously assumed. Therefore, a fin having a geometric aspect ratio of 7/8 and an area of 2.57 sq. in., if placed on the model in the same position as those previously tested, should produce the same inclining moment and angle of breakdown as the anticipated prototype fin. The fin area of 2.57 sq. in. is considered to be the minimum area that will accomplish this desired result.

G. Virtual mass calculations

The basic formula for calculating the virtual mass effect of a projecting surface with dimensions as indicated in the sketch is:

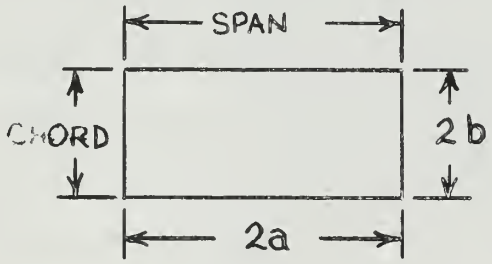

$$M_v = \frac{2 \times \rho \times \pi \times a^2 \times b^2}{\sqrt{a^2 + b^2}}$$

For the purpose of this thesis, only the relative effect of non-geometrically similar fins on the virtual mass as compared with the virtual mass of geometrically similar fins is of interest. For this purpose, only the ratio $\frac{a^2 \times b^2}{\sqrt{a^2 + b^2}}$ need be considered.

For the geometrically similar fin, $a = 0.894$, $b = 0.447$, and $\frac{a^2 \times b^2}{\sqrt{a^2 + b^2}} = 0.160$. For the recommended low aspect ratio fin

developed in section F of this appendix having an aspect ratio of 7/8 and an area of 2.57 sq. in., a = 0.750 and b = 0.857. The ratio

$$\frac{a^2 \times b^2}{\sqrt{a^2 + b^2}} = 0.360.$$

Therefore, the relative effect on virtual mass of the low aspect ratio fin will be $\frac{0.360}{0.160} = 2.26$ times as great as the virtual mass effect of a geometrically similar fin.

H. Development of a dimensionless pumping rate coefficient C_q for boundary layer control

For purposes of applying the data developed in this thesis to other experimental work in boundary layer control with other fins having different areas and different speeds through the water, a dimensionless pumping rate coefficient C_q was developed in the following manner. The observed pumping rate in GPM was divided by the total area of the fin to which boundary layer was applied and the speed of the fin through the water. For the dimensions of Q, s′, and V_m given in the list of symbols, this coefficient becomes

$$C_q = \frac{0.19 \times Q}{s' \times V_m}$$

In the runs made in which boundary layer control was employed, the total area of the geometrically similar fin was reduced by the area closed by the end pieces and the area closed at the trailing edge where the upper and lower surfaces were soldered together. The area applied in the above equation was $s' = 1.08$ sq. in. The model speed was 1.829 knots. This gives a value of $C_q = 0.0967 \times Q$.

Applying this to the values of Q used in the runs employing boundary layer control gives the following values of the dimensionless pumping

rate coefficient:

For Q = 1.5 GPM, $C_q = 0.145$

For Q = 0.75 GPM, $C_q = 0.0725$

APPENDIX C

REFERENCES

(1) Flipse, J. E., "Stabilizer Performance on S.S. MARIPOSA and S.S. MONTEREY," paper presented at May 3, 1957 meeting of SNAME.

(2) Allan, J. F., "The Stabilization of Ships by Activated Fins," INA, vol. 87, 1945, pp. 123-149.

(3) Chadwick, J. H., Jr., "On the Stabilization of Roll," Trans. SNAME, vol. 63, 1955, pp. 237-269.

(4) Jacobs, E. N., and Sherman, A., "Airfoil Section Characteristics as Affected by Variations of the Reynolds Number," NACA Report No. 586, 1937.

(5) Mandel, P., "Some Hydrodynamic Aspects of Appendage Design," Trans. SNAME, vol. 61, 1953, pp. 464-496.

(6) Chadwick, J. H., Jr., "The Anti-Roll Stabilization of Ships by Means of Activated Fins," Technical Report No. 1, Part A, Contract N6-onr-25129, Department of Electrical Engineering, Stanford University, 1953.

(7) Hagen, G. R., "Feasibility Studies of Roll Stabilization of the USS BOSTON (CAG-1)," DTMB Report 950, September, 1955.

(8) Reid, E. G., Applied Wing Theory, New York, McGraw-Hill Book Company, Inc. c1933, pp. 98-101.

(9) Glauert, H., The Elements of Aerofoil and Airscrew Theory, New York, The MacMillan Company, 1943, pp. 146-147.

(10) Schlichting, H., Boundary Layer Theory, New York, Pergamon Press, 1955.

(11) Abkowitz, M. A., and Pauling, J. R., Jr., "The Ship Model Towing Tank at M.I.T.," Trans. SNAME, vol. 61, 1953, pp. 65-97.

(12) Porter, W. R., "Angular Motion Instrumentation for Model Seaworthiness Testing," M.I.T. Naval Engineer's Thesis, June, 1955.

(13) Lewis, E. V., and Jacobs, W. R., "Preliminary Study of the Influence of Controlled Fins on Ship Pitching and Heaving," ETT Note No. 379, February 8, 1957, pp. 5-8.

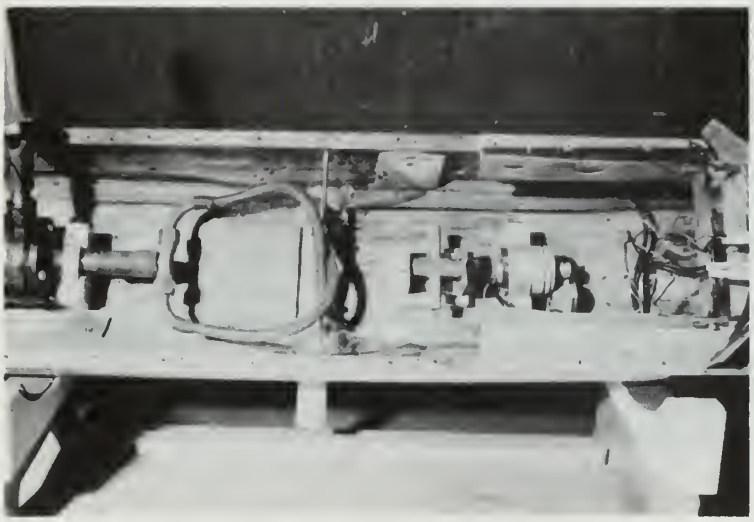

FIGURE V

Interior view of model with towing bracket removed.

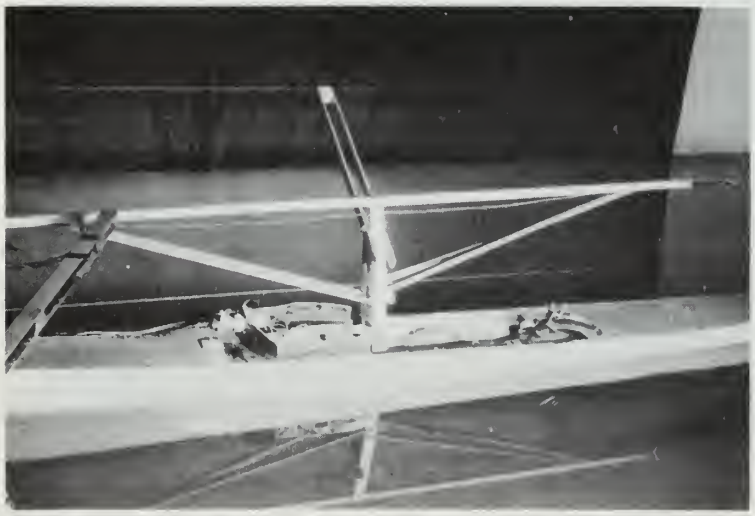

FIGURE VI

Model in the towing tank.

FIGURE VII

Sanborn Recorder, 400 cycle generating and rectifying equipment.

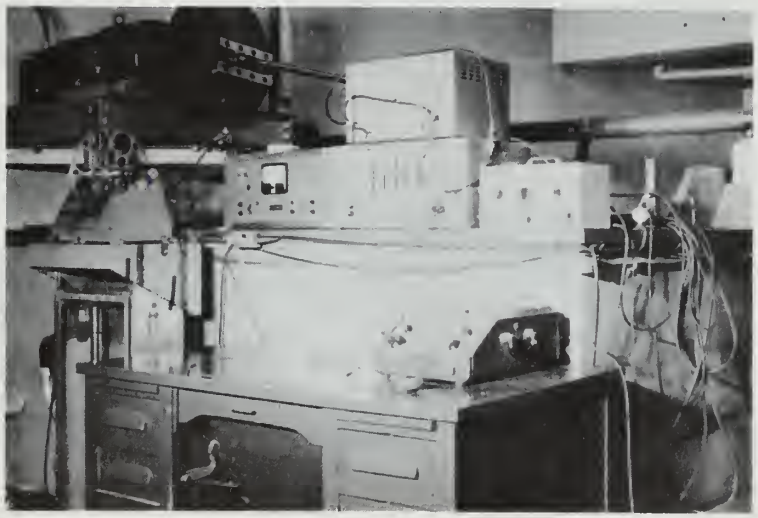

FIGURE VIII

View of the dynamometer end of the towing tank.

FIGURE IX

Low aspect ratio fin installed on the model.

FIGURE X

Geometrically similar fin installed on the model,

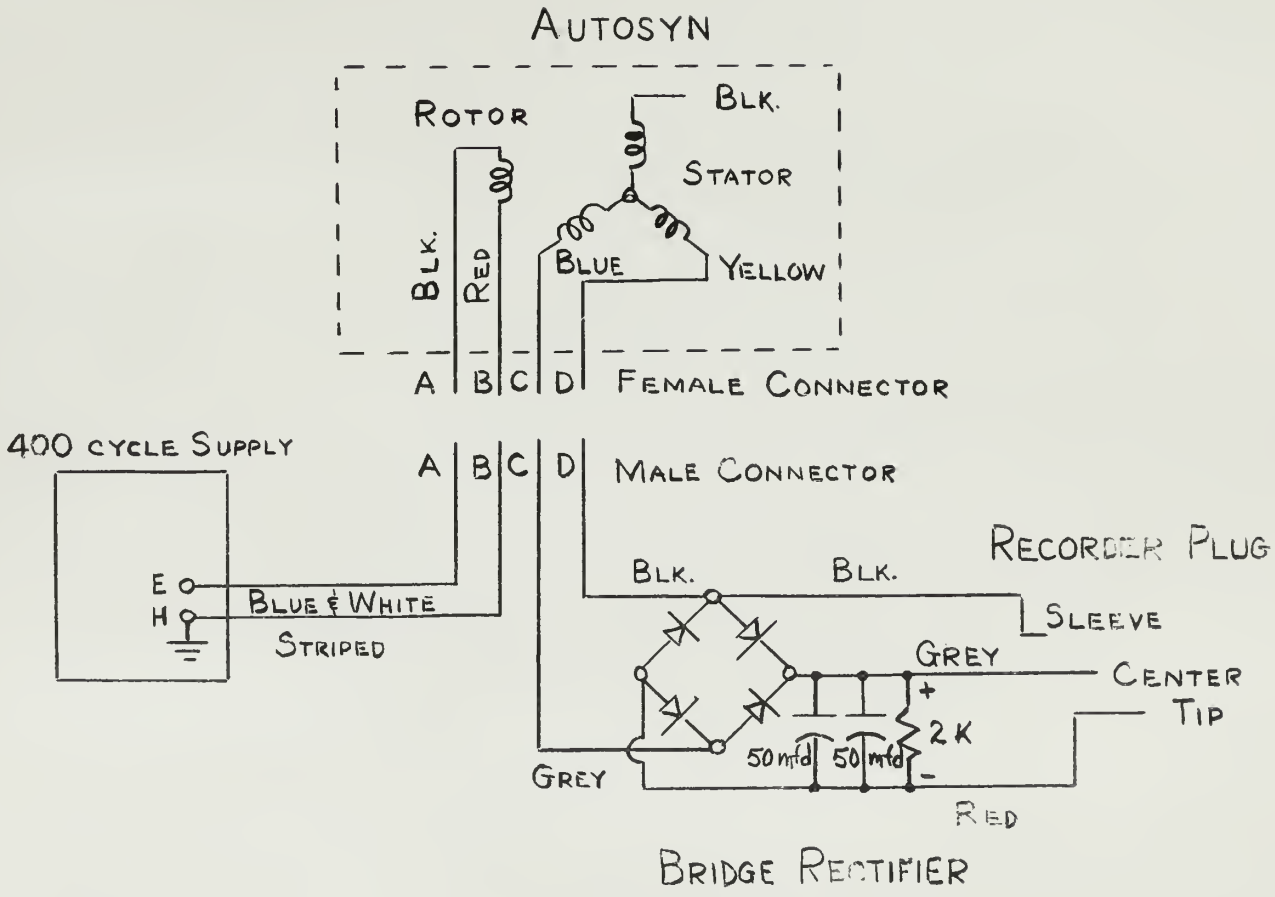

FIGURE XI

.WIRING DIAGRAM OF 400 CYCLE POWER SUPPLY,

AUTOSYN, RECTIFIER, AND SANBORN D.C. AMPLIFIER CONNECTIONS